

# Recognizing Micro-expression in Video Clip with Adaptive Key-frame Mining

Min Peng<sup>1,2,†</sup>, Chongyang Wang<sup>3,†\*</sup>, Yuan Gao<sup>4</sup>, Tao Bi<sup>3</sup>, Tong Chen<sup>5</sup>, Yu Shi<sup>1</sup>, Xiang-Dong Zhou<sup>1</sup>

**Abstract**—As a spontaneous expression of emotion on face, micro-expression is receiving increasing focus. Whilst better recognition accuracy is achieved by various deep learning (DL) techniques, one characteristic of micro-expression has been not fully leveraged. That is, such facial movement is transient and sparsely localized through time. Therefore, the representation learned from a long video clip is usually redundant. On the other hand, methods utilizing the single apex frame require manual annotations and sacrifice the temporal dynamic information. To simultaneously spot and recognize such fleeting facial movement, we propose a novel end-to-end deep learning architecture, referred to as Adaptive Key-frame Mining Network (AKMNet). Operating on the raw video clip of micro-expression, AKMNet is able to learn discriminative spatio-temporal representation by combining the spatial feature of self-exploited local key frames and their global-temporal dynamics. Empirical and theoretical evaluations show advantages of the proposed approach with improved performance comparing with other state-of-the-art methods.

**Index Terms**—Adaptive Key-frame Mining, Deep Learning, Micro-Expression Recognition

## I. INTRODUCTION

PREVIOUSLY, as an obvious facial movement pattern, macro-expression is one of the dominant modalities for non-contact emotion recognition. Macro-expression is consciously expressed by people and typically lasts from a half to four seconds, which can be easily perceived by normal people [1]. In addition to understanding the macro-expression, many works have been conducted on identifying and recognizing them (for review, see [2] [3]). However, it has been pointed out by several studies [4] [5] that macro-expression could be misleading and leveraged to conceal the genuine emotion. In contrast, micro-expression is found to be conveyed

unconsciously as a transient (last less than half second) and subtle facial movement, while being proved to reveal the underlying emotions [5]. Due to previously stated reasons, the recognition of micro-expression has become a new popularity in the affective computing community and boosted a wide range of real-world applications [4] [6] [7].

Research on automatic recognition of micro-expression first took the advantage of abundant works on macro-expression recognition, where the popular pipeline is, e.g., image preprocessing including normalization and cropping etc., and feature engineering followed up by classification with machine learning methods. To name a few, Zhao et al. [8] [16] adopted the Local Binary Pattern (LBP) onto the three orthogonal planes (LBP-TOP) of micro-expression clip, to extract the dynamic facial texture feature and applied Support Vector Machine (SVM) to conduct the classification. Another adaption of LBP-TOP is seen in the work by Huang et al [34], where the Spatio-Temporal Completed Quantization Patterns (STCLQP) is proposed to consider sign, magnitude and orientation as feature components. Vector quantization is adopted to obtain compact and discriminative codebooks in spatiotemporal domain. To reduce the information redundancy existed in LBP-TOP features, Wang et al. [9] further designed an algorithm called LBP-Six Intersection Points (LBP-SIP) to replace LBP-TOP for the feature extraction process. After this, Wang et al [33] proposed a Tensor Independent Color Space (TICS) to replace the traditional RGB color space. Their experiments found that perceptual color spaces like CIELab and CIELuv are better than RGB to represent the dynamic texture information of micro-expression. On the other hand, Li et al. [10] conducted a comparison among LBP-TOP, Histogram of Oriented Gradients (HOG) and Histogram of Image Gradient Orientation (HIGO) on their feature extraction capability on micro-expression videos.

Except for these evolved from previous researches on facial macro expression recognition, methods proposed for generic video analysis from wider computer vision community have also inspired the research on facial micro-expression recognition. More recently, Optical Flow [11] has been harnessed to enable better temporal feature extraction of micro-expression. Happy et al [35] studied the temporal feature extraction of facial micro movements with Fuzzy Histogram of Optical-Flow Orientation (FHOFO) features. Liu et al. [12] divided the face into 36 regions based on the facial action coding system [38], and captured the subtle facial movement in video clip by computing the Main Directional Mean Optical-flow (MDMO) feature of each area. In their following

Manuscript submitted for review in September 2020.

<sup>1</sup>Chongqing Institute of Green and Intelligent Technology, Chinese Academy of Sciences, Chongqing, China. (e-mail: {pengmin, shiyu, zhuxiangdong}@cigit.ac.cn).

<sup>2</sup>Chongqing School, University of Chinese Academy of Sciences, Chongqing, China.

<sup>3</sup>UCL interaction centre, University College London, London, United Kingdom. (e-mail: {chongyang.wang.17, t.bi}@ucl.ac.uk).

<sup>4</sup>Department of information technology, Uppsala University, Uppsala, Sweden. (email: alex.yuan.gao@it.uu.se)

<sup>5</sup>School of Electronic and Information Engineering, Southwest University, Chongqing, China. (email: c\_tong@swu.edu.cn)

<sup>†</sup>Equal contribution.

<sup>\*</sup>Correspondence author.

work, it is also tried to add sparsity into such feature extraction to reduce redundancy [36]. Later, Xu et al. [13], similarly based on Optical Flow, designed a fine-grained temporal alignment method and an optical-flow direction optimization strategy for the feature extraction of micro-expression clips. So far, accuracies on micro-expression recognition achieved with these feature-engineering methods are slightly higher than the level of what the human expert can perform. However, sophisticated pre-processing stages and feature design are always needed, thus these previous works on micro-expression are more suitable for the scenario of off-line analysis.

One commonality of the methods above is the use of video clips as the data input for micro-expression recognition. However, recent researches have challenged such practice from several perspectives. The micro-expression clips provided in the two prevalent benchmarks, namely CASME I [14] and CASME II [15], are manually segmented, providing the location of onset, apex and offset frames. The number of frames between the onset and offset frames of each video clip ranges from 9 to more than 100. As a result, temporal normalization technique like the Temporal Interpolation Method (TIM) [17] has become a common prior step for many existing methods, which was originally designed to cope with video clips of different lengths. However, such method would disturb the temporal order of the original video clip to some extent (e.g., making a temporal process longer/shorter), while a better model should accept input with varying temporal lengths. Additionally, empirical experiments [18] [19] [20] show that most of the frames within a micro-expression clip are not contributing to the recognition, which can be referred to as redundant frames. Such result is also due to the fact that micro-expression itself is transient and expressed within several localized frames. Moreover, two recent studies [21] [22] supported this argument by showing the advantage of using the apex frame alone for the recognition instead of the entire (pre-segmented) video clip. Nevertheless, two notable disadvantages of apex-frame-based methods are: i) the need for extra manual annotation of the apex-frame, which reduces the end-to-end integrity of a system; ii) the loss of the temporal pattern of micro-expression, which could hinder the generalization capability of a system on the recognition of a same micro-expression type across different participants. A recent work by Peng et al. [27] proposed to improve the latter issue by integrating the temporal information adjacent to the apex frame. In [41], the author tried to enrich the feature from the apex frame by searching for useful extra information with genetic algorithms. However, manual annotations of the apex frame are still needed.

In this work, we propose an end-to-end deep learning architecture named **Adaptive Key-frame Mining Network** (AKMNet) to adaptively select the optimal key frames and learn the spatio-temporal features for micro-expression recognition given video clips of different durations. Specifically, the AKMNet has three modules, namely the traversal-processing, adaptive key-frame mining and spatio-temporal fusing modules. The traversal-processing module is a spatial feature extraction unit, which processes

each frame of the input video in a traversal manner, aimed to create a sequence of spatial features. Then, in key-frame mining module, a temporal subset comprising key frames is learned by searching through such feature sequences. This is achieved using a constrained optimization process with designed loss functions. Finally, in spatio-temporal fusing module, this temporal subset will be further processed to acquire the spatio-temporal features, based on which classification is performed. During the training, all these three modules are integrated to conduct end-to-end learning for micro-expression recognition. The location of key frames, which should contribute most to the recognition, may change given different video clips and micro-expression categories.

To the best of our knowledge, this is the first deep learning study deliberated to enable automatic learning of the optimal temporal subset from a video clip for the micro-expression recognition. Also, the design of all the modules in the proposed network is independent to the length of the input video clip. In other words, our model tolerates micro-expression clips of different lengths. The contribution of this paper can be summarized into three folds:

-A novel deep learning architecture, referred to as AKMNet, is proposed to be tolerative to micro-expression clips with various lengths.

-A trainable adaptive key-frame mining algorithm is proposed to automatically find the optimal temporal subset for micro-expression recognition. To the best of our knowledge, this is the first time for such temporal-subset learning module to be used for this problem.

-Through extensive experiments, the proposed AKMNet is proved to be effective for micro-expression recognition in video clips with noticeably improved performance.

## II. RELATED WORKS

Following the feature-engineering methods mentioned in the last section, the past three years have witnessed a growing response in micro-expression community towards the boom of deep learning in computer vision community. Various deep neural networks have been used in several case studies therein. Without hand-crafted feature engineering, an end-to-end neural network model is capable of classification or prediction by learning from large sets of high dimensional (and low-level representation of) data [23]. For the research on micro-expression, efforts have been made to adapt several successful CNN and RNN models from the wider computer vision domain to solve problems in this scenario.

First, researchers have focused on extracting representation from the entire micro-expression clip (including frames between the onset frame and offset frame). To name a few, Peng et al. [18] proposed to use 3D-CNN to learn representation from the optical-flow sequence transformed from such clip, while SVM was used for the final classification. The proposed architecture possesses two streams, which were aimed to consume the data in different original framerates from the two benchmark datasets (CASME I/II), and each stream was also mitigated to only have 4 convolutional layers each followed by a pooling layer in order to alleviate the over-fitting

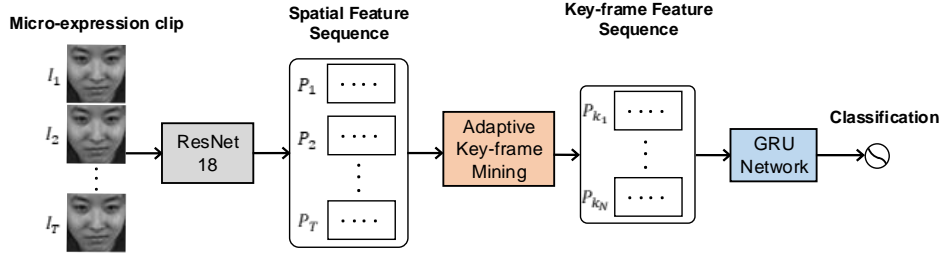


Fig. 1. Overview of proposed AKMNet. The network first conducts spatial feature extraction with ResNet-18 on the micro-expression clip input with frames number of  $T$ . Then  $N$  selected frames will be generated from the adaptive key-frame mining module which are further processed by a bi-GRU network to learn the spatio-temporal feature. The classification is conducted on the top of such feature.

risk. Through end-to-end implementation and testing on CASMEI/II, such method achieved a best f1-score of 0.6667 with 3-fold cross validation, which is around 10% higher than previously state-of-the-art methods ([12] [13]). Considering the temporal dynamic of the video data, Qian et al [24] proposed an architecture with convolutional and recurrent layers. Together with the full video clip, the optical flow feature was also extracted at each timestep for a given period to provide richer temporal information. However, the accuracy they achieved was somehow limited, which may be due to the use of a complex network on the small datasets. In the two studies mentioned above, two popular network architectures (3D-CNN and CNN-RNN) originally used for video classification have been tested on micro-expression datasets, while the accuracy achieved is comparable if not better than previous hand-crafted feature engineering methods, under a practical end-to-end manner with higher real-life impact.

However, except for the limited size of datasets, another important challenge existed is the redundancy introduced by unimportant frames within each video clip of micro-expression. Toward this issue, recent studies [21] [22] have explored the feasibility of using the apex frame of each video clip alone for the recognition, where the intensity of a micro-expression is believed to reach the highest. Both of the works proved that not all the frames of a micro-expression clip contribute to the recognition. Following up such finding, researchers begin to use the apex frame to conduct micro-expression recognition. Peng et al [19] proposed to use transfer learning to aid the micro-expression recognition on apex frames by pre-training on macro-expression data. As suggested in this work, micro-expression recognition on the apex frame opened a way to transfer knowledge learned from data of macro-expression, since both tasks are strongly relevant and operated on static images. Another work by Wang et al [20] [25] proposed to use attention mechanism to help the network focus on most informative spatial areas of the apex frame as micro-expression is localized on small areas of face. Later on, another study by Peng et al [27] found that integrating the spatial information of an apex frame with temporal information of the frames adjacent to it produced higher generalization ability across different datasets. One important limitation we found of the apex-frame based studies is the lack of a generic method to locate the essential frame e.g., the apex frame. Some studies [21] [22] located apex frame based on spatial or spectral feature engineering, while the rest [19] [20] [27] relied on annotations.

In this paper, to avoid the redundancy of using all the frames in the micro-expression clip and the dependency on manual annotations of essential frames, we propose to automatically learn the optimal subset of frames that contribute most to the recognition performance. Our method combines the automatic subset-searching, spatio-temporal representation fusion and recognition, by proposing an end-to-end network called AKMNet. Specially, we also aim to design an integrated end-to-end network that accepts micro-expression clips with varying lengths and automatically learns the temporal subset thereon, on which the spatio-temporal feature is spontaneously extracted. In the next section, the methodology is described in detail to show how we achieve this.

### III. METHODOLOGY

In this section, we first illustrate the overall architecture of the proposed AKMNet. We show how the proposed network is designed to automatically learn the key frames from a video clip of micro-expression of varying lengths. Then we describe in detail the proposed computational algorithms used in the adaptive key-frame mining module within AKMNet.

#### A. Overview of AKMNet

Micro-expression is a transient and temporally localized facial movement indicating the internal emotion of a person. Therefore, the number of frames informative to the recognition of micro-expression is limited. Additionally, the duration of a micro-expression clip varies across different subjects, even for the same emotion. Such temporal nature and individual differences manifest that it is essential to first find the most informative frames, then to conduct the recognition thereon. We believe, first, for a video clip of micro-expression, richer information are stored in some key frames in comparison with other redundant frames. Secondly, the distribution of the key frames could be sparse, thus each key frame could be connected by several redundant frames.

An overview of the proposed AKMNet is shown in Figure 1. Given a video input  $\mathbf{V} = \{I_1, I_2, \dots, I_T\}$ , with  $I_T$  represents the  $T$ -th frame, the AKMNet first extracts the spatial feature for each frame using a ResNet-18 network [31]. The generated feature sequence is  $\mathbf{F} \in \mathbb{R}^{T \times C \times W \times H}$  where  $\mathbf{F} = \{P_1, P_2, \dots, P_T\}$ .  $P_T \in \mathbb{R}^{C \times W \times H}$  is the spatial feature extracted from the  $T$ -th frame  $I_T$ , where  $C, W, H$  are the number of channels, width and height respectively. The same ResNet-18 network is shared during the spatial-feature extraction across frames. Such is to i)

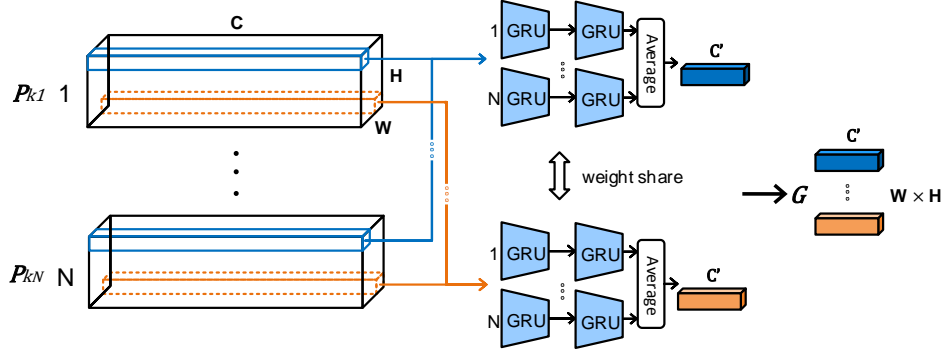


Fig. 2. The pixel-wise recurrent processing on key-frame feature sequence with bi-GRU networks. Each bi-GRU network processes a sequence of pixel-wise feature vectors extracted from all the key frames.

ensure the feature extracted from each frame provides the same level of information; ii) tolerate clip input of different lengths; iii) reduce the number of trainable parameters so as to alleviate the overfitting risk on the small micro-expression dataset. The ResNet-18 network was first initialized using the ImageNet [37] and further pre-trained with a macro-expression dataset named AffectNet [39]. Such is aimed to transferring the ability of ResNet from generic image classification to facial expression recognition as well as to alleviate the over-fitting risk. Details for the adaptive key-frame mining module is given in the next subsection. Such module produces a feature sequence subset of  $N$  frames that are expected to be most informative for the recognition, denoted as  $\mathbf{F}^{Key} \in \mathbb{R}^{N \times C \times W \times H}$ ,  $\mathbf{F}^{Key} = \{\mathbf{P}_{k_1}, \mathbf{P}_{k_2}, \dots, \mathbf{P}_{k_N}\}$ . These key frames are listed following their original temporal order in the spatial feature sequence  $\mathbf{F}$ , i.e. we have  $1 \leq k_1 < k_N \leq T$ . The number of key frames  $N$  is adaptively changed given different input clips.

As shown in Figure 2, the key-frame feature sequence  $\mathbf{F}^{Key} = \{\mathbf{P}_{k_1}, \mathbf{P}_{k_2}, \dots, \mathbf{P}_{k_N}\}$  is processed by a bi-directional GRU network (bi-GRU) [32] to extract the temporal feature. Specially, the bi-GRU network is employed to conduct a **pixel-wise recurrent processing**. A single bi-GRU network is operating on a sequence of feature pixels with size of  $N \times C$ , extracted from the same position across all the key frames. As the size of a spatial feature  $\mathbf{P}_{k_N}$  is  $C \times W \times H$ , we have totally  $W \times H$  bi-GRU networks in order to process all the feature pixel across all the frames. In this way, the temporal feature is extracted without pooling. Such is also aimed to maintain the spatial information, as for micro-expression such information is essential. All the bi-GRU networks share the same set of learnable parameters, so as to help reduce parameter size and tolerate clip inputs of different lengths. For the bi-GRU network, given a sequential input at spatial position  $(i, j)$  across all key frames  $\mathbf{F}_{(i,j)}^{Key} = \{\mathbf{P}_{k_1}^{(i,j)}, \mathbf{P}_{k_2}^{(i,j)}, \dots, \mathbf{P}_{k_N}^{(i,j)}\}$ , the output  $h_n$  at  $n$ -th key frame  $\mathbf{P}_{k_n}^{(i,j)}$  is computed as

$$h_n = (1 - z_n) * h_{n-1} + z_n * \tilde{h}_n, \quad (1)$$

$$z_n = \sigma(\mathbf{W}_z \cdot [h_{n-1}, \mathbf{P}_{k_n}^{(i,j)}]), \quad (2)$$

$$\tilde{h}_n = \tanh(\mathbf{W}_{\tilde{h}} \cdot [\sigma(\mathbf{W}_r \cdot [h_{n-1}, \mathbf{P}_{k_n}^{(i,j)}]) * h_{n-1}, \mathbf{P}_{k_n}^{(i,j)}]), \quad (3)$$

where  $[\cdot]$  represent the stacking of different vectors,  $*$  is

element-wise multiplication,  $\sigma$  is sigmoid activation,  $h_{n-1}$  is the output of the last key frame.  $\mathbf{W}_z$ ,  $\mathbf{W}_{\tilde{h}}$  and  $\mathbf{W}_r$  are the trainable weight matrices of the bi-GRU network. The output of each bi-GRU network is the average of the output  $h_n$  across all key frames. Such output from each bi-GRU network is concatenated to produce the **key-frame spatio-temporal representation**  $\mathbf{G} \in \mathbb{R}^{C' \times W \times H}$ , where  $C'$  is channels number of the feature vector produced by each bi-GRU network.

In our end-to-end training, a softmax layer is adopted thereon to conduct the final classification. The loss function here can be written as

$$\mathcal{L}_c = -\sum_{m=1}^M \mathbf{1}\{y^{(\mathbf{G})} = m^*\} \log \frac{e^{\mathbf{W}_m^* \mathbf{G}}}{\sum_{m=1}^M e^{\mathbf{W}_m \mathbf{G}}}, \quad 1 < m \leq M, \quad (4)$$

where,  $M$  is the number of the total classes,  $m^*$  indicates the groundtruth class of current input video clip,  $y^{(\mathbf{G})}$  is the classified category identity of input feature  $\mathbf{G}$ ,  $\mathbf{W}$  is weight vector between output layer and previous layer.  $\mathbf{1}\{\cdot\}$  is the eigenfunction, when  $\{\cdot\}$  is true it will return 1, and 0 vice versa.

### B. Adaptive Key-frame Mining Module

Here, we describe in detail how the key-frame mining module works. In general, the key-frame mining module learns a function  $f_{AKM}: \mathbf{F} \rightarrow \mathbf{F}^{key}$ . A demonstration of the key-frame mining module is provided in Figure 3. As shown, the input to such module the feature sequence  $\mathbf{F} \in \mathbb{R}^{T \times C \times W \times H}$  is first processed with a global spatial pooling to produce a pooled feature sequence  $\bar{\mathbf{F}} \in \mathbb{R}^{T \times C}$ . That is, we compress each feature map  $\mathbf{P}_t \in \mathbb{R}^{C \times W \times H}$  in the sequence  $\mathbf{F}$  into a  $C \times 1$  feature vector  $\bar{\mathbf{P}}_t$ ,  $t \in \{1, 2, \dots, T\}$ , which contains compact spatial information of each frame.

In order to acquire the key-frame sequence, a three-step key-frame mining module is proposed. First, a **local self-attention learning step** is adopted, where a coarse attentional weight  $\alpha_t$  is assigned to each feature vector  $\bar{\mathbf{P}}_t$ . Second, based on these attentional weights computed in the first step, a global feature vector  $\tilde{\mathbf{P}}$  is produced by aggregating all the feature vectors. Thereon, a fine-grained weight for each feature vector is acquired by computing the cosine correlation between each feature vector and the global feature vector. We call such as **global correlation learning step**. Finally, based on these correlation values, a sparse binary correlation vector  $\mathbf{B}$  is learned using a global sparsity and maximum mean-margin

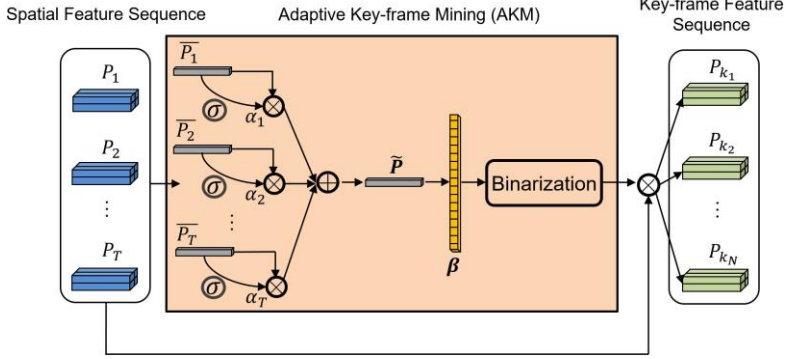


Fig. 3. The adaptive key-frame mining module.

loss function. This is referred to as **sparse selection step**. These three steps proposed for the key-frame mining module are empirically justified in the next section to understand their individual impact.

In the local self-attention learning step, the local weight  $\alpha_t$  for each frame feature input  $\bar{P}_t$  is computed through a fully-connected layer with sigmoid activation function as

$$\alpha_t = \sigma(\mathbf{W}^T \bar{P}_t), \quad (5)$$

where  $\sigma$  is sigmoid activation function,  $\mathbf{W}^T$  is the trainable weight matrix for this layer.

In the global correlation learning step, we first acquire the global feature vector  $\tilde{P}$  by aggregating all the input feature vectors and respective local self-attentional weights as

$$\tilde{P} = \sum_{t=1}^T \alpha_t \bar{P}_t. \quad (6)$$

Then, the fine-grained weight  $\beta_t$  for each feature vector  $\bar{P}_t$  is computed based on cosine correlation as

$$\beta_t = \frac{\bar{P}_t \cdot \tilde{P}}{\|\bar{P}_t\|_2 \|\tilde{P}\|_2}, \quad (7)$$

where  $\|\cdot\|_2$  denotes the L2-norm.

Finally, in the sparse selection step, we implement the concept reasoned earlier that most frames in a video clip of micro-expression are redundant while the most informative frames are sparsely localized. Thus, we add sparsity to the weight vector  $\{\beta_1, \beta_2, \dots, \beta_T\}$ . Inspired by the binarization process presented in the binary neural network [26], we compute the binary index vector  $B \in \{0,1\}^{T \times 1}$  as

$$B_t = \begin{cases} 1, & \beta_t > \frac{1}{T} \sum_{t=1}^T \beta_t \\ 0, & \beta_t \leq \frac{1}{T} \sum_{t=1}^T \beta_t \end{cases}, \quad t \in \{1, 2, \dots, T\}, \quad (8)$$

where the location of key frames are marked with number 1, and 0 vice versa. With index vector  $B$ , the key frame feature sequence  $\mathbf{F}^{key}$  is acquired by

$$\mathbf{F}^{key} = \mathbf{F} \odot B, \quad (9)$$

where  $\odot$  denotes the tensor-fraction product and is conducted along the temporal dimension of the original feature sequence  $\mathbf{F}$ . To further enable the learning of the fine-grained weight  $\beta_t$  and the sparsenization process, we propose to use a **Global Sparsity and Maximum Mean-Margin (GS-MMM)** loss function. The first part of global sparsity loss is written as

$$\mathcal{L}_{GS} = \max(0, \sum(B) - 1), \quad (10)$$

where  $\max(\cdot)$  and  $\sum(\cdot)$  are the computation for maximum and sum respectively. When  $\mathcal{L}_{GS}$  is reduced, we make sure at least one key frame is selected. Another part of maximum mean-margin loss is written as

$$\mathcal{L}_{MMM} = C - \left( \frac{1}{\sum(B)} \sum_{t=1}^T B_t \beta_t - \frac{1}{T - \sum(B)} \sum_{t=1}^T (1 - B_t) \beta_t \right), \quad (11)$$

where  $C$  is set to 2 given that the value of fine-grained weight  $\beta_t$  is within the range of cosine function. This loss function is aimed to further help discriminate the key frames from the others by assigning higher weights thereon, while avoid the trivial solution possibly led to by  $\mathcal{L}_{GS}$ . Thereon, the GS-MMM loss function is written as

$$\mathcal{L}_{GS-MMM} = \lambda_1 \mathcal{L}_{GS} + \lambda_2 \mathcal{L}_{MMM}, \quad (12)$$

where  $\lambda_1$  and  $\lambda_2$  are the weight constants controlling the impact of each loss respectively. During the end-to-end training of the AKMNet, to combine the Equation 4 and 12, the final loss function  $\Omega$  to be reduced can be written as

$$\Omega = \mathcal{L}_c + \mathcal{L}_{GS-MMM}. \quad (13)$$

In training, the network needs to learn the optimal key-frame subset that lead to the minimum loss  $\Omega$ , which shall also give the best classification performance. Through back propagation, the trainable weight matrices in the ResNet-18 and bi-GRU networks are updated. In the next subsection, we discuss how to transform such adaptive key-frame mining approach into a trainable block of the deep learning network.

### C. Weight Update Strategy

Normally, gradient descent is used to update a neural network, which expects all the computation conducted in the network to be differentiable and convex. However, the adaptive key-frame mining module described in the last subsection appears to be a non-convex process. Specifically, the calculation of binary index vector  $B$  does not allow gradient computation. To make the process trainable, we develop an alternative minimization method to update the Equation 8 and 9.

We first define that, during the back-propagation, the gradient passed from the next layer to the layer of  $\mathbf{F}^{key}$  is denoted as  $\frac{\partial \Omega}{\partial \mathbf{F}^{key}}$ . According to the chain rule, the gradient update for Equation 9 can be written as

$$\frac{\partial \Omega}{\partial \mathbf{F}} = \frac{\partial \Omega}{\partial \mathbf{F}^{key}} \cdot \frac{\partial \mathbf{F}^{key}}{\partial \mathbf{F}} = \frac{\partial \Omega}{\partial \mathbf{F}^{key}} \cdot B. \quad (14)$$

vice versa

$$\frac{\partial \Omega}{\partial \mathbf{B}} = \frac{\partial \Omega}{\partial \mathbf{F}^{key}} \cdot \frac{\partial \mathbf{F}^{key}}{\partial \mathbf{B}} = \frac{\partial \Omega}{\partial \mathbf{F}^{key}} \cdot \mathbf{F}. \quad (15)$$

For Equation 8, the computation of index vector  $B$  produces constant value, which does not allow gradient computation. Therefore, we modify such computation by replacing the constant value with the original fine-grained weight value respectively. The Equation 8 can be re-written as

$$B_t = \begin{cases} \beta_t, & \beta_t > \frac{1}{T} \sum_{t=1}^T \beta_t \\ 0, & \text{otherwise} \end{cases}, t \in \{1, 2, \dots, T\}. \quad (16)$$

Then, according to the chain rule, the gradient update for Equation 8 can be written as

$$\frac{\partial \Omega}{\partial \beta} = \begin{cases} \frac{\partial \Omega}{\partial \mathbf{B}} \cdot \frac{\partial \mathbf{B}}{\partial \beta} = \frac{\partial \Omega}{\partial \mathbf{B}}, & \beta_t > \frac{1}{T} \sum_{t=1}^T \beta_t \\ 0, & \text{otherwise} \end{cases}, t \in \{1, 2, \dots, T\}. \quad (17)$$

With Equation 14-17, the back-propagation for the weight updating of the proposed adaptive key-frame mining module is enabled. Such module is integrated into the network as shown in Figure 1.

#### D. End-to-end Training of AKMNet

In AKMNet, the recognition of micro-expression given a video clip input comprises three stages: i) the traversal spatial-feature extraction with ResNet-18 for the input video clip; ii) the adaptive key-frame mining with the proposed module, where a sequence of key feature maps is produced that are most valuable for the recognition; iii) learning the pixel-wise temporal features with the bi-GRU network followed by feature concatenation, and classification. The end-to-end learning is enabled for the entire network. The training scheme is written in Algorithm 1.

---

#### Algorithm 1 The End-to-End Training of AKMNet.

---

1. **Input:**  $\mathbf{V} = \{\mathbf{I}_1, \mathbf{I}_2, \dots, \mathbf{I}_T\}$
2. **while** training **do**
3. Extract the sequence of spatial feature  $\mathbf{F} = \{\mathbf{P}_1, \mathbf{P}_2, \dots, \mathbf{P}_T\}$  from the input  $\mathbf{V}$ , using the ResNet-18 network initialized with ImageNet and pre-trained with larger macro-expression datasets.
4. With  $\mathbf{F}$ , use the adaptive key-frame mining module to produce the index vector  $\mathbf{B} \in \{\mathbf{0}, \mathbf{1}\}^{T \times 1}$  as Eq. 8.
5. With  $\mathbf{B}$ , generate the sequence of key-frame feature maps  $\mathbf{F}^{key} = \{\mathbf{P}_{k_1}, \mathbf{P}_{k_2}, \dots, \mathbf{P}_{k_N}\}_{k_1 \geq 1}^{k_N \leq T}$  as Eq. 9.
6. With  $\mathbf{F}^{key}$ , first compute the temporal feature with a bi-GRU Network. Then produce a spatio-temporal feature matrix  $\mathbf{G}$  after feature concatenation.
7. In the classification layer, compute loss  $\Omega$  as Eq. 13.
8. Based on  $\Omega$ , update the bi-GRU network, AKM module and ResNet-18 network with back propagation.
9. **End**
10. **Output:** classification result  $\mathbf{m}$

---

## IV. EXPERIMENTS AND EVALUATIONS

In this section, we evaluate proposed approach using several theoretical analyses and empirical experiments. The data pre-processing is first described, followed by experimental settings. Finally, we report the results and discussions.

TABLE I DETAILS OF CASME I AND CASMEII

Feature	CASME I	CASME II
Clips number	189	255
Camera speed	60fps	200fps
Frame length	9-86	24-141
Frame length var	123	515
Average facial resolution	167×137	257×225
Categories	Happiness, Surprise, Tense, Disgust, Sadness, Fear, Repression, Contempt	Happiness, Surprise, Disgust, Sadness, Fear, others

#### A. Data Preparation

For our experiments, two benchmark datasets are used, namely CASME I [14] and CASME II [15]. Details for these two datasets are reported in Table I. To utilize the two datasets together, we merged their original classes into four categories, namely positive (happiness), negative (disgust, sadness, and fear), surprise and others (contempt, tense and repression).

During training, the number of video clips of each class will be equalized by resampling them according to the class comprising largest number of clips. An augmentation we also conduct here is *cropping*, where for each video clip, each frame will be first resized to 144×144 and then cropped at random positions to make new images with size of 128×128. Data left for testing will be directly resized to 128×128 without any extra processing. Here we need to note that the length of each video clip remains unchanged.

#### B. Experimental Set-up

ResNet-18 [31] is adopted for spatial feature extraction in the proposed AKMNet. The detailed architecture of the adopted ResNet-18 is shown in Table II. Given a video clip input  $\mathbf{V} = \{\mathbf{I}_1, \mathbf{I}_2, \dots, \mathbf{I}_T\}$  with length  $T$ , the output is  $\mathbf{F} \in \mathbb{R}^{T \times 512 \times 4 \times 4}$ . In order to alleviate the overfitting risk and aid the convergence of the training with micro-expression data, an initialization is conducted for the ResNet-18 using ImageNet dataset [37], which is further pre-trained with a macro-expression dataset named AffectNet [39]. For the four categories of positive, negative, supervise and others, we each randomly sample 1000 pictures from this dataset to conduct the pre-training.

For the adaptive key-frame mining module, a key-frame feature subset  $\mathbf{F}^{key} = \{\mathbf{P}_{k_1}, \mathbf{P}_{k_2}, \dots, \mathbf{P}_{k_N}\}$  is generated, with  $1 \leq k_1 < k_N \leq T$ . The number of key frames  $N$  is decided

TABLE II ARCHITECTURE OF THE ADOPTED RESNET-18

Layer	Kernel Parameter	Output Size
Conv1	5 × 5, 64	64 × 64 × 64
Conv2 x	$[3 \times 3, 64] \times 2$	64 × 32 × 32
Conv3 x	$[3 \times 3, 128] \times 2$	128 × 16 × 16
Conv4 x	$[3 \times 3, 256] \times 2$	256 × 8 × 8
Conv5 x	$[3 \times 3, 512] \times 2$	512 × 4 × 4

through network learning, and is not dependent on the input video length of  $T$ . Due to individual differences, even for the same micro-expression type video clips with the same length may finally harvest key-frame subsets of different lengths. For Equation 12,  $\lambda_1$  and  $\lambda_2$  are set to 0.1 and 1 respectively.

For the spatio-temporal learning part, at each input spatial position across all the frames, a two-layer bi-GRU network is used. Namely, the input for each bi-GRU network is a feature map with size of  $N \times 512$ , while the respective output dimension is  $C' = 64$ . The output of all the timestep of such network is averaged to be the output of each spatial position. The output of all the bi-GRU networks is concatenated together to form the spatio-temporal feature matrix  $\mathbf{G} \in \mathbb{R}^{64 \times 4 \times 4}$ . This feature matrix is flattened into a vector and used as an input to the final fully-connected softmax layer for classification. A drop-out layer with probability set to 0.5 is added before the softmax layer.

For the training of AKMNet, we set the mini-batch size to 8 with initial learning rate to 1e-3. The learning rate is adapted using a scheme named Cosine Annealing LR [29], with a minimum set to 1e-8. The number of maximum epochs is set to 40. For the back propagation of networks, the stochastic gradient descent (SGD) [30] is used, with momentum set to 0.9 and weight decay set to 5e-4. The leave-one-subject-out cross validation (LOSO) is used.

In the control groups, for LBP-TOP, LBP-SIP, STCLQP, HIGO and FHOFO, the number of frames of all the video clips are normalized to 20. Specially, for LBP-TOP, LBP-SIP and STCLQP, the radius of the X, Y and temporal axis are set to 3 with the neighbor size set to 8. For LBP-TOP, the uniform LBP implementation is used to extract the feature. For STCLQP, the level of orientation estimation N and quantization level T are set to 16 and 4 respectively. For HIGO, the number of bins is set to 8. For FHOFO, we extract the optical-flow information based on [40], while the number of fine-grained bins is set to 36, the coarse-grained bins is set to 8 and the variance value is set to 10. For MDMO, the number of frames of each video clip composed CASME I and CASME II is normalized to 64 and 128 respectively, while for each frame the facial area is equally divided into 36 regions. Similarly, for this method, the optical-flow feature is extracted using the implementation proposed in [40]. For the above methods, the linear SVM is used as classifier in the end.

### C. Comparison Experiment

Results for the comparison between proposed AKMNet and other state-of-the-art methods are given in Table III. The first part of comparison methods were based on feature engineering and shallow classifiers. The three methods in the middle of the table used different deep learning architectures on the apex frame or also on the frames adjacent to the apex frame. In general, the best performance is achieved by the proposed AKMNet (accuracies of 0.7619 and 0.6863 on CASME I and II respectively), operated on raw video clips without using any prior knowledge about the temporal property (e.g., locations of the apex frame).

It is observed on CASME I that, the deep learning method

TABLE III RECOGNITION RESULTS (%) ON CASME I/II DATASETS IN THE COMPARISON EXPERIMENT

Methods	CASME I	CASME II
LBP-TOP [8]	0.5820	0.5412
LBP-SIP [9]	0.5926	0.5490
STCLQP [34]	0.6349	0.5886
HIGO [10]	0.6085	0.5686
FHOFO [35]	0.6614	0.6078
MDMO [12]	0.6720	0.6353
Macro2Micro (Apex frame) [19]	0.6825	0.5961
Micro Attention (Apex frame) [20]	0.6931	0.6157
ATNet (Apex and adjacent frames) [27]	0.7090	0.6275
<b>AKMNet</b>	<b>0.7619</b>	<b>0.6863</b>

based on the apex frame lead to better performance than traditional approaches using full video clips. However, such advantage is not seen on CASME II, where MDMO achieved a better result of 0.6353 than Macro2Micro and Micro Attention methods operated on apex frames. One explanation could be that, given the cameras used for CASME II equipped with a higher framerate (200FPS VS. 60 FPS as used for CASME I), informative temporal patterns of micro-expression were captured and contained across several frames in a video clip, instead of only on the apex frame. Such is further supported by the slightly better results achieved with ATNet (accuracy of 0.6275), where frames adjacent to the apex frame were added during modeling. These results imply the importance of temporal patterns of micro-expression contained in the video clip data. Accordingly, the best result achieved by AKMNet can be owe to its adaptive key-frame mining module, which can search for an optimal temporal subset for the recognition. We make efforts to further prove this in the next subsection.

### D. Justification of the Adaptive Key-frame Mining Module

In order to justify the effectiveness and robustness of the proposed AKMNet in terms of its adaptive key-frame mining design, we conduct a justification experiment here. We use **AKMNet<sup>va</sup>** to denote a dedicated variant of AKMNet where the only difference is the absence of the adaptive key-frame mining module. That is, spatial feature sequence  $\mathbf{F}$  generated by ResNet-18 is processed by the bi-GRU network directly. In detail, variants we designed here includes:

- **AKMNet<sup>va</sup>-all**, where all the frames in an input video clip are used.

- **AKMNet<sup>va</sup>-norm  $\beta$** , where an input video clip is first normalized with TIM [17] to be a new clip with frames number  $\beta \in \{16, 32, 64, 128\}$ .

- **AKMNet<sup>va</sup>-random**, where for each input video clip, given the number of key frames  $N$  learned by the default AKMNet respectively, the same number of frames is randomly sampled to be the input of this model. The result reported here is the average performance after five repeated random samplings.

Results are reported in Table IV. In comparison with **AKMNet<sup>va</sup>-norm  $\beta$** , comparable if not better result is achieved by **AKMNet<sup>va</sup>-all** (accuracy of 0.6825 and 0.6275 on CASME I and II respectively). This suggests that, for some video clips,

TABLE IV RECOGNITION RESULTS (%) ON CASME I/II DATASETS IN THE JUSTIFICATION EXPERIMENT

Methods	CASME I	CASME II
AKMNet <sup>va</sup> - <i>all</i>	0.6825	0.6275
AKMNet <sup>va</sup> - <i>norm16</i>	0.6702	0.6170
AKMNet <sup>va</sup> - <i>norm32</i>	0.6984	0.6078
AKMNet <sup>va</sup> - <i>norm64</i>	0.7090	0.6157
AKMNet <sup>va</sup> - <i>norm128</i>	0.7354	0.6039
AKMNet <sup>va</sup> - <i>random</i>	0.7143	0.6275
<b>AKMNet</b>	<b>0.7619</b>	<b>0.6863</b>

the temporal normalization can indeed harm the recognition. Also, given the fluctuation of performances of AKMNet<sup>va</sup>-*norm*  $\beta$  under different  $\beta$ , the classification accuracy is generally reduced when the number of normalized frames input to the model is too small (16) or too many (128). This could be due to that i) many frames in a micro-expression video clip are redundant or even harmful to the classification performance; ii) but there exists an underlying subset of several frames that can lead to the best performance.

In comparison with these results, an intermediate performance is achieved by AKMNet<sup>va</sup>-*random*. Unlike the TIM method that maintains the temporal order of all the frames in the input video clip, such performance achieved by a random sampling suggests that the informative frames are disconnectedly spread in the clip. On CASME II, the increase of frame numbers for AKMNet<sup>va</sup>-*norm*  $\beta$  lead to an improvement of performance. This could also due to the higher frame rate of the video clip contained in CASME II, which comprised more informative frames of the presented micro-expression. The different performance fluctuation trends of AKMNet<sup>va</sup>-*norm*  $\beta$  observed on the CASME I/II implies the impact of the frame rate of cameras used for data collection. Especially, when the sampling rate of TIM (e.g., 128) is higher than the original frame rate (e.g., the 60 FPS of CASME I), redundant information could be introduced while the performance is dropped. A discussion about generating fixed number of frames using TIM is seen in several works [10, 12, 13, 18]. However, given the individual differences in the presentation of micro-expression, the length of underlying optimal temporal subset of micro-expression should be varying. To the best of our knowledge, this study is the first to leverage the temporal characteristic of micro-expression under different temporal scales. In this experiment, the best performance on the two datasets is achieved by the proposed AKMNet that adaptively learns to find the optimal subset of frames in the input video clip.

### E. Ablation Experiment

The function of the adaptive key-frame mining module is realized through three steps, namely local self-attention learning, global correlation learning and sparse selection. It can be noticed that all these steps have some overlap on each other, while it remains unknown if our proposal of combining them is the best approach for the key-frame mining. Here, we run an ablation study on the three steps by creating three meaningful

TABLE V RECOGNITION RESULTS (%) ON CASME I/II DATASETS IN THE ABLATION EXPERIMENT

Methods	CASME I	CASME II
AKMNet- <i>s12</i>	0.6931	0.5922
AKMNet- <i>s13</i>	0.6984	0.6275
AKMNet- <i>s23</i>	0.7196	0.6118
<b>AKMNet-<i>s123</i></b>	<b>0.7619</b>	<b>0.6863</b>

variants of the AKMNet:

- **AKMNet-*s12***, where the sparse selection step is absent.
- **AKMNet-*s13***, where the global correlation learning step is absent.
- **AKMNet-*s23***, where the local self-attention learning step is absent.

The proposed method used in other subsections is now referred to as **AKMNet-*s123***, as to help the discrimination among them. Results are reported in Table V. We can see that, by removing one component from the proposed key-frame mining module, all the three variants lead to reduced performance than our proposed method. Such result justified our use of a combination of the three steps. On both datasets, variants equipped with step three of sparse selection (AKMNet-*s13* and AKMNet-*s23*) have comparatively better results than the one without it (AKMNet-*s12*). This result may once again verify that the key frames of micro-expression are sparsely spread in a video clip, while a sparse selection step could help the network to get rid of redundant frames instead of reserving them with lower weights.

### F. Is the Annotated Apex Frame the ‘Most Informative’?

So far, we have shown the advantage of the proposed AKMNet in comparison with methods that directly leverage expert-annotated apex frame, and the adjacent frames as input. An important study still missing is to understand the relationship between the key frames learned by the AKMNet and the respective apex frame annotated by human experts. It was supported by a series of studies [19-22, 27] that, for a micro-expression video clip, the apex frame shall contribute most to the recognition performance. Given such, we suppose the key frames learned by the AKMNet for each video clip may comprise the apex frame and several relevant frames. In this subsection, we analyze the key frames learned by AKMNet for each micro-expression video clip to understand this. First, for each dataset, we calculate the ratio of video clips where i) the apex frame is included in the key frames learned by the AKMNet (denoted as Ratio); ii) the apex frame is included and assigned the highest weight among the key frames (denoted as Ratio<sup>W</sup>). Results are reported in Table VI. We can see that, as expected, for most video clips (>50%) of the two datasets, the apex frame annotated by human experts is also included as the

TABLE VI RATIOS (%) OF VIDEO CLIPS IN CASME I/II DATASETS WHERE THE APEX FRAME IS LEARNED AS THE KEY FRAME AND ASSIGNED THE HIGHEST WEIGHT

Dataset	Ratio	Ratio <sup>W</sup>
CASME I	0.5833	0.1
CASME II	0.7086	0

TABLE VII RECOGNITION RESULTS (%) OF MACRO2MICRO MODEL WITH INPUT OF APEX FRAMES AND MAX-KEY FRAMES RESPECTIVELY

Input	CASME I	CASME II
Apex frame	0.6825	0.5961
Max-key frame	<b>0.7090</b>	<b>0.6118</b>

key frame learned by AKMNet. However, it is interesting to learn that there are only ~10% video clips in CASME I where the apex frame is given the highest weight, while in CASME II there is no such video clip. In other words, mostly, the proposed data-driven AKMNet does not find the apex frame to be most informative for the micro-expression recognition. Such could be due to the error that human experts may commit during the apex-frame annotation, resulting in a temporal distance (a number of frames) between the apex frame and underlying most-informative key frame. Alternatively, human experts may perceive the micro-expression differently from the data-driven model, which only aimed to increase the recognition performance. To empirically verify if the key frame assigned with the highest weight (denoted as max-key frame) learned by AKMNet being more informative than the apex frame annotated by human experts, we run another experiment with Macro2Micro model [19]. Under the same experimental setting, we run the model on apex frames and max-key frames separately for CASME I/II. Results are reported in Table VII. As we can see, better performances are achieved using the max-key frame learned by AKMNet, instead of using the expert-annotated apex frame. Such result empirically verified the existence of the very informative key frame of each video clip, which, however, could get ignored by human experts during the apex-frame annotation. Here need to note that this experiment is not challenging the idea of using the *apex frame* for micro-expression recognition, but suggesting that the expert annotation of such frame may not be that accurate for a recognition purpose. In Figure 4, we show the distribution of the distance between the apex frame and max-key frame of each video clip in the CASME I/II datasets. It should be noted that, given the framerates of the two datasets (200 VS. 60 fps), distances computed for CASME II are normalized by dividing with a factor of 3.33. We can see that most apex frames are located within the distance of less than 10 frames from the max-key frame. This may imply again the error that human experts could commit during the annotation process, which is

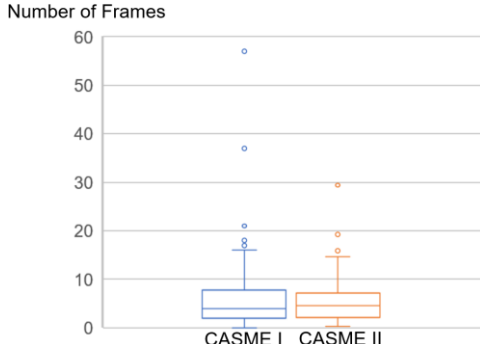


Fig. 4. Boxplots of the distribution of the distance between the max-key frame and apex frame in each video clip for CASMEI/II..

not obvious given the short distance between the annotated apex frame and the more informative max-key frame.

#### G. Generalization Experiment

Experiments conducted above have shown the effectiveness of the proposed approach on micro-expression recognition with video clips. The design of AKMNet is actually not only limited to the recognition of micro-expression, but is believed to be applicable to the more generic scenario where the events-of-interest are sparsely located in a data sequence. Here, we adopt a facial macro-expression benchmark dataset CK+ [28] to test the applicability of AKMNet outside the micro-expression recognition scenario. In the CK+ dataset, 327 video clips captured from 118 participants were labelled with 7 macro-expression categories, namely happiness, anger, sadness, fear, disgust, contempt and surprise. In our experiment, we run a hold-out validation where data from 80% of the participants are used for training with the rest 20% participants left out for testing. Five variants of the AKMNet created in the justification experiment are used here to aid the comparison, namely  $\text{AKMNet}^{\text{va}}\text{-all}$  and  $\text{AKMNet}^{\text{va}}\text{-norm } \beta$ ,  $\beta \in \{16, 32, 64, 128\}$ . Results are summarized in Table IX. The best performance is still achieved by the proposed AKMNet, in comparison with the methods taking in all the input frames or applying the temporal interpolation at different scales. This result shows the generalization ability of the proposed approach on a relevant scenario, even if some intrinsic characteristics of the target are not fully leveraged during the modeling e.g., the larger size of available data and higher spatial intensify of the facial macro-expression. We believe higher recognition performances can be achieved by modifying the AKMNet according to these factors. On the other hand, the method taking in all the input frames ( $\text{AKMNet}^{\text{va}}\text{-all}$ ) has better performance than the ones using temporal interpolations ( $\text{AKMNet}^{\text{va}}\text{-norm}\beta$ ). One reason for such result could be that the higher facial movement intensify of macro-expression left more continuous information across all the frames, which could be harmed by the use of temporal interpolation.

TABLE IX RECOGNITION RESULTS (%) ON CK+ DATASET IN THE GENERALIZATION EXPERIMENT

Methods	Accuracy
$\text{AKMNet}^{\text{va}}\text{-all}$	0.9280
$\text{AKMNet}^{\text{va}}\text{-norm}16$	0.9063
$\text{AKMNet}^{\text{va}}\text{-norm}32$	0.9016
$\text{AKMNet}^{\text{va}}\text{-norm}64$	0.8881
$\text{AKMNet}^{\text{va}}\text{-norm}128$	0.8837
<b>AKMNet</b>	<b>0.9344</b>

## V. CONCLUSIONS

The recognition of micro-expression has reached a new era where researchers started to leverage the intrinsic characteristics of such facial expression. Specifically, the subtle intensity and short duration of micro-expression have been harnessed during the method development. In this paper, we have focused on the transient presentation of micro-expression that it is usually

sparingly located in a video clip. An end-to-end network architecture named AKMNet equipped with an adaptive key-frame mining module has been proposed. The module was designed to learn an optimal temporal subset from the spatial feature sequence of an input video clip. Our evaluation with two benchmark datasets, namely CASMEI and CASME II, has showed noticeable improvements achieved by the AKMNet over state-of-the-art methods. A further justification study has verified the effectiveness of the proposed adaptive key-frame mining module, in comparison with the variants using all frames, different temporal interpolations and random samplings of the video clip. In the ablation study, we verified the combination of the three steps in the key-frame mining module, which produced the best performance than other implementations. In the study comparing expert-annotated apex frame and model-learned max-key frame, we empirically showed the advantage of using the latter one as the single-frame input. This study also revealed the possible error that could be committed by human experts during data annotation, and also the perception difference between the human expert and data-driven AKMNet. In the final experiment, a comparable generalization ability of the AKMNet on a relevant macro-expression benchmark dataset was also witnessed. Given the proposed AKMNet being a data-driven approach, future works may seek to collaborate with human experts to improve its further efficacy on micro-expression recognition and enrich the theoretical space of micro-expression, and explore applications in relevant domains.

#### ACKNOWLEDGMENT

This work is funded by the National Natural Science Foundation of China (Grant No. 61802361 and Grant No. 61806185). Chongyang Wang is supported by the UCL Overseas Research Scholarship (ORS) and Graduate Research Scholarship (GRS).

## REFERENCES

[1] Paul, Ekman. "Emotions revealed: recognizing faces and feelings to improve communication and emotional life." NY: OWL Books (2007).

[2] C. A. Corneanu, M. O. Simón, J. F. Cohn and S. E. Guerrero, "Survey on RGB, 3D, Thermal, and Multimodal Approaches for Facial Expression Recognition: History, Trends, and Affect-Related Applications," in *IEEE Transactions on Pattern Analysis and Machine Intelligence*, vol. 38, no. 8, pp. 1548-1568, 1 Aug. 2016.

[3] E. Sariyanidi, H. Gunes and A. Cavallaro, "Automatic Analysis of Facial Affect: A Survey of Registration, Representation, and Recognition," in *IEEE Transactions on Pattern Analysis and Machine Intelligence*, vol. 37, no. 6, pp. 1113-1133, 1 June 2015.

[4] Porter, Stephen , and L. T. Brinke . "Reading Between the Lies: Identifying Concealed and Falsified Emotions in Universal Facial Expressions." *Psychological Science* 19.5(2008):508-514.

[5] Ekman, Paul. "Lie catching and microexpressions." *The philosophy of deception* 1.2 (2009): 5.

[6] Russell, Tamara A , E. Chu , and M. L. Phillips . "A pilot study to investigate the effectiveness of emotion recognition remediation in schizophrenia using the micro-expression training tool." *British Journal of Clinical Psychology* 45.Pt 4(2011):579-583.

[7] Weinberger, and Sharon. "Airport security: Intent to deceive?" *Nature* 465.7297(2010):412-5.

[8] M. Pietikainen, G. Zhao, Xiaobai Li and T. Pfister, "Recognising spontaneous facial micro-expressions," in *2011 IEEE International Conference on Computer Vision (ICCV 2011)*, Barcelona, 2011 pp. 1449-1456. Doi: 10.1109/ICCV.2011.6126401

[9] Wang, Yandan , et al. "LBP with Six Intersection Points: Reducing Redundant Information in LBP-TOP for Micro-expression Recognition." *Accv Springer*, Cham, 2014.

[10] X. Li et al., "Towards Reading Hidden Emotions: A Comparative Study of Spontaneous Micro-Expression Spotting and Recognition Methods," in *IEEE Transactions on Affective Computing*, vol. 9, no. 4, pp. 563-577, 1 Oct.-Dec. 2018.

[11] Sun, Deqing , S. Roth , and M. J. Black . "A Quantitative Analysis of Current Practices in Optical Flow Estimation and the Principles Behind Them." *International Journal of Computer Vision* 106.2(2014):115-137.

[12] Y. Liu, J. Zhang, W. Yan, S. Wang, G. Zhao and X. Fu, "A Main Directional Mean Optical Flow Feature for Spontaneous Micro-Expression Recognition," in *IEEE Transactions on Affective Computing*, vol. 7, no. 4, pp. 299-310, 1 Oct.-Dec. 2016.

[13] F. Xu, J. Zhang and J. Z. Wang, "Microexpression Identification and Categorization Using a Facial Dynamics Map," in *IEEE Transactions on Affective Computing*, vol. 8, no. 2, pp. 254-267, 1 April-June 2017.

[14] Wen-Jing Yan, Q. Wu, Yong-Jin Liu, Su-Jing Wang and X. Fu, "CASME database: A dataset of spontaneous micro-expressions collected from neutralized faces," 2013 10th IEEE International Conference and Workshops on Automatic Face and Gesture Recognition (FG), Shanghai, 2013, pp. 1-7.

[15] Yan, Wen Jing , et al. "CASME II: An Improved Spontaneous Micro-Expression Database and the Baseline Evaluation." *Plos One* 9.1(2014):e86041.

[16] G. Zhao, M. Pietikainen. (2007). "Dynamic Texture Recognition Using Local Binary Patterns with an Application to Facial Expressions," *IEEE Transactions on Pattern Analysis & Machine Intelligence*, 29(6):915.

[17] T. Pfister, Xiaobai Li, G. Zhao and M. Pietikäinen, "Recognising spontaneous facial micro-expressions," 2011 International Conference on Computer Vision, Barcelona, 2011, pp. 1449-1456.

[18] Peng, Min et al. "Dual temporal scale convolutional neural network for micro-expression recognition." *Frontiers in psychology* 8 (2017): 1745.

[19] M. Peng, Z. Wu, Z. Zhang and T. Chen, "From Macro to Micro Expression Recognition: Deep Learning on Small Datasets Using Transfer Learning," 2018 13th IEEE International Conference on Automatic Face & Gesture Recognition (FG 2018), Xi'an, 2018, pp. 657-661.

[20] Wang, Chongyang et al., "Micro-Attention for Micro-Expression Recognition." *Neurocomputing* (2020).

[21] Lioing, Sze-Teng et al. "Less is more: Micro-expression recognition from video using apex frame." *Signal Processing: Image Communication* 62 (2018): 82-92.

[22] Y. Li, X. Huang and G. Zhao, "Can Micro-Expression be Recognized Based on Single Apex Frame?" 2018 25th IEEE International Conference on Image Processing (ICIP), Athens, 2018, pp. 3094-3098.

[23] Miotto, Riccardo et al. (2017). "Deep learning for healthcare: review, opportunities and challenges." *Briefings in bioinformatics*.

[24] H. Khor, J. See, R. C. W. Phan and W. Lin, "Enriched Long-Term Recurrent Convolutional Network for Facial Micro-Expression Recognition," 2018 13th IEEE International Conference on Automatic Face & Gesture Recognition (FG 2018), Xi'an, 2018, pp. 667-674.

[25] M. Peng, C. Wang and T. Chen, "Attention Based Residual Network for Micro-Gesture Recognition," 2018 13th IEEE International Conference on Automatic Face & Gesture Recognition (FG 2018), Xi'an, 2018, pp. 790-794.

[26] Lin, Xiaofan , C. Zhao , and W. Pan . "Towards Accurate Binary Convolutional Neural Network." *NIPS* 2017.

[27] M. Peng, C. Wang, T. Bi, Y. Shi, X. Zhou and T. Chen, "A Novel Apex-Time Network for Cross-Dataset Micro-Expression Recognition," 2019 8th International Conference on Affective Computing and Intelligent Interaction (ACII), Cambridge, United Kingdom, 2019, pp. 1-6.

[28] P. Lucey, J. F. Cohn, T. Kanade, J. Saragih, Z. Ambadar and I. Matthews, "The Extended Cohn-Kanade Dataset (CK+): A complete dataset for action unit and emotion-specified expression," 2010 IEEE Computer Society Conference on Computer Vision and Pattern Recognition - Workshops, San Francisco, CA, 2010, pp. 94-101.

[29] Loshchilov, Ilya , and F. Hutter . "SGDR: Stochastic Gradient Descent with Warm Restarts." (2016).

[30] Williams, Ronald J. . "Simple statistical gradient-following algorithms for connectionist reinforcement learning." *Machine Learning* 8.3-4(1992):229-256.

[31] He, Kaiming et al. "Deep residual learning for image recognition." In *Proceedings of the IEEE conference on computer vision and pattern recognition (CVPR)*, pp. 770-778. (2016).

[32] Chung, Junyoung , et al. "Empirical Evaluation of Gated Recurrent Neural Networks on Sequence Modeling." *Eprint Arxiv* (2014).

[33] Wang, Su-Jing et al. "Micro-expression recognition using color spaces." *IEEE Transactions on Image Processing* 24, no. 12 (2015): 6034-6047.

[34] Huang, Xiaohua et al. "Spontaneous facial micro-expression analysis using spatiotemporal completed local quantized patterns." *Neurocomputing* 175 (2016): 564-578.

[35] S. L. Happy and A. Routray, "Fuzzy Histogram of Optical Flow Orientations for Micro-Expression Recognition," in *IEEE Transactions on Affective Computing*, vol. 10, no. 3, pp. 394-406, 1 July-Sept. 2019.

[36] Y. Liu, B. Li and Y. Lai, "Sparse MDMO: Learning a Discriminative Feature for Spontaneous Micro-Expression Recognition," in *IEEE Transactions on Affective Computing*.

[37] J. Deng, W. Dong, R. Socher, L. Li, Kai Li and Li Fei-Fei, "ImageNet: A large-scale hierarchical image database," 2009 IEEE Conference on Computer Vision and Pattern Recognition, Miami, FL, 2009, pp. 248-255.

[38] Ekman, Rosenberg. *What the face reveals: Basic and applied studies of spontaneous expression using the Facial Action Coding System (FACS)*. Oxford University Press, USA, (1997).

[39] A. Mollahosseini, B. Hasani and M. H. Mahoor, "AffectNet: A Database for Facial Expression, Valence, and Arousal Computing in the Wild," in *IEEE Transactions on Affective Computing*, vol. 10, no. 1, pp. 18-31, 1 Jan.-March 2019.

[40] Liu, Ce. "Beyond pixels: exploring new representations and applications for motion analysis." *Diss. Massachusetts Institute of Technology*, 2009.

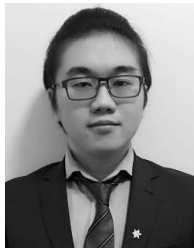
[41] Jin, Qiu-Shi, Huang-Chao Xu, Kun-Hong Liu, Sze-Teng Lioing, Y. S. Gan, and Shu-Wen Su. "GA-APEXNET: Genetic Algorithm in Apex Frame Network for Micro-expression Recognition System." In *Journal of Physics: Conference Series*, vol. 1544, no. 1, 2020.



**Min Peng** is a Ph.D. student at Chongqing School, University of Chinese Academy of Sciences, China. He is also a research fellow at Intelligent Security Center, Chongqing Institute of Green and Intelligent Technology, Chinese Academy of Sciences, China. In 2017, he received the M.S. degree in affective computing from Southwest University, China. His research interests include machine learning, computer vision and affective computing.



**Chongyang Wang** is a Ph.D. candidate at UCL interaction centre, University College London, United Kingdom, under the supervision of Prof. Nadia Bianchi-Berthouze and Dr. Nicholas D. Lane. In 2017, he received the B.E. degree in electronic and information engineering from Southwest University, China. His current research topics include computer vision and developing new ubiquitous body sensing technology to support smart physical rehabilitation.



**Yuan Gao** is a Ph.D. candidate at Department of Information Technology, Uppsala University, Sweden under the Supervision of Prof. Ginevra Castellano, and Prof. Danica Kragic Jensfelt. In 2016, he received his M.Sc. in Algorithms and Machine Learning from University of Helsinki, Finland. His current research topics include deep reinforcement learning for robotics and deep learning-based approaches for perception and control of social robotics.



**Tao Bi** is a Ph.D. candidate under the supervision of Prof. Nadia Bianchi-Berthouze at UCL interaction centre, University College London, United Kingdom, where he also obtained his M.S. Degree in HCI in 2017. His research interests include Human-Computer Interaction (HCI) and Affective Computing.



**Tong Chen** received the B.E. degree in communication engineering from The Second Artillery Command Institute, China, in 2002, the M.S. degree in digital sound and vision processing from University of Wales, United Kingdom, in 2006, and the Ph.D. degree from Cranfield University, United Kingdom, in 2013. He is currently a professor in Southwest University, China. His research interests include image/signal processing, machine learning, and affective computing.



**Yu Shi** is the director of Center on Research of Intelligent Security Technology, CIGIT, Chinese Academy of Sciences, China. He leads a team for core technology and industrial application research in Computer Vision and Pattern Recognition area.

He has published more than 20 patents, and has obtained 4 patent licenses. He is the West Light A Class awarded by Chinese academy of sciences.



**Xiang-Dong Zhou** is an associate professor at CIGIT, Chinese Academy of Sciences, China. He received the B.S. degree in Applied Mathematics and the M.S. degree in Management Science and Engineering both from National University of Defense Technology, China, the Ph.D. degree in pattern recognition and artificial intelligence from the Institute of Automation, Chinese Academy of Sciences, China, in 1998, 2003 and 2009, respectively.

He was a postdoctoral fellow at Tokyo University of Agriculture and Technology, Japan from March 2009 to March 2011. His research interests include handwriting recognition and ink document analysis.